Chapter-I

1.1 Introduction

Over the last few decades, multiferroics have drawn increasing interest due to their potential for multiple performances for device application in a single material. Multiferroic materials are multifunctional materials which exhibit at least two or more of the ferroic properties such as ferro/antiferro-electricity, ferro/antiferro-magnetism and ferroelasticity simultaneously with some coupling between two ferroic properties. Multiferroics have stimulated great interest of researchers due to the potential applications for devices such as sensors, actuators, transducers and memories [Hill (2000); Eerenstein et al. (2006)]. In ferroelectrics, spontaneous polarization is present which can be switched hysteretically by applied electric field. Ferromagnetic materials have spontaneous magnetization which can be switched hysteretically by an applied magnetic field. In antiferromagnetic materials, ordered magnetic moments cancel each other entirely within each magnetic unit cell whereas in ferrimagnetic materials cancellation is incomplete so that some magnetic moment is present. Ferroelastic materials possess a spontaneous deformation which can be switched hysteretically by an applied stress [Ramesh (2009)]. In multiferroics, coexistence of these ferroic properties produces additional interactions such as magneto-electricity, magneto-elasticity etc and thus provides more degree of freedom for designing novel devices. A schematic diagram of these interactions [Spaldin and Fiebig (2005)] is shown in Fig.1.1. In magneto-electric multiferroics, polarization (P) can be directly controlled by applying magnetic field (H) and magnetization

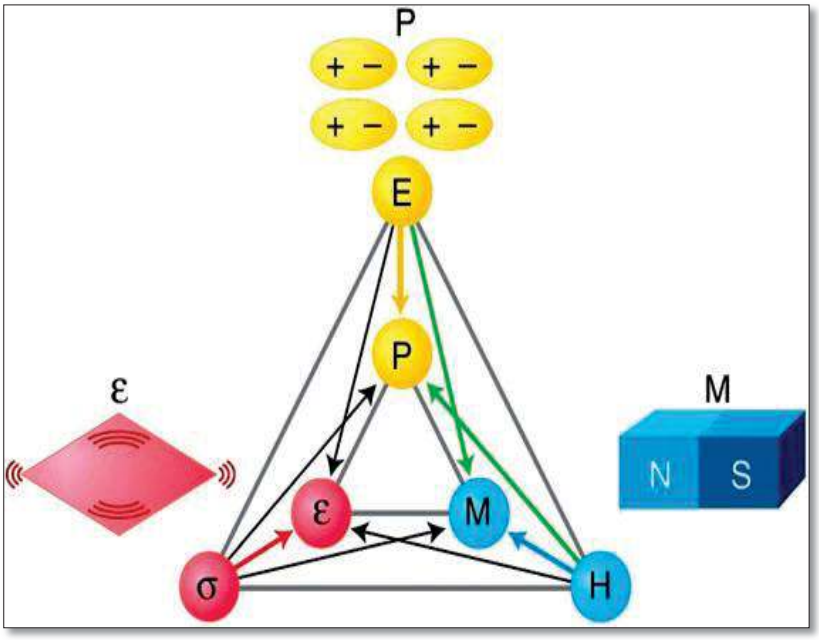

Fig.1.1. Schematic diagram of phase control in ferroics and coupling of different types of ferroic orders in multiferroic materials [after Spaldin and Fiebig (2005)].

(M) can be directly controlled by applying electric field (E) as shown in Fig.1.1. Similarly, in magneto-elastic materials strain (ε) can be directly produced by applying magnetic field (H) and magnetization (M) by applying stress (σ). Recently, great interests in multiferroics are shown by researchers due to interesting physics involved and large demand from industries for multifunctional materials [Hill (2000); Khomskii (2006)]. However, these multiferroics are very rare and only few have been found in nature or synthesized in the laboratory due to contradictory requirement of primary ferroic orders [Hill (2000); Hill et al. (2002); Feibeg (2005); Khomskii (2006); Ramesh et al. (2007)]. First-principles density functional theory calculations by Cohen [Cohen (1992)] show that hybridization between B-site cation and O-anion is essential for ferroelectric distortion in ABO_3 perovskites. Vacant d-orbital (d^0) at B-site cations soften the orbital overlapping between B-site cation and O-anion which results in to ferroelectricity [Cohen and Krakauer (1992)]. In contrast, unpaired electrons in the d-orbital (d^n) of B-site cations are required for the existence of magnetic ordering but reduce its tendency of hybridization with oxygen ions which is crucial for the appearance of ferroelectricity. Most of the single phase multiferroics show very low value [Nan et al. (2008)] of magnetoelectric (ME) coefficient. Appearance of ME response below room temperature is other drawback of these single phase multiferroics [Kumar et al. (1998)]. Only few single phase multiferroics such as $BiFeO_3$ or $LuFe_2O_4$ exhibit ME response above room temperature but ME-coefficient is even low [Wang et al. (2009)].

Multiferroic composites may be the substitute for these single phase multiferroics where coupling between two ferroic properties is obtained by indirect interactions [Suchtelen (1972); Skinner et al. (1978)]. Multiferroic composite may be formed by taking the suitable combinations of ferroelectric phases (e.g. $BaTiO_3$, $Pb(Zr_xTi_{1-x})O_3$, $PbTiO_3$ etc) and magnetic phases (e.g. $NiFe_2O_4$, $La_{0.7}Sr_{0.3}MnO_3$, $CoFe_2O_4$, $NiZnFe_2O_4$, etc) [Boomgaard et al. (1976); Nan et al. (2008)]. Multiferroic composite may exhibit very large ME-coefficient as high as ~10^2V/cm-Oe above room temperature which is not observed in single phase materials [Nan et al. (2008)].

The present thesis deals with a comprehensive study of (1-x)$Bi(Ni_{1/2}Ti_{1/2})O_3$-x$PbTiO_3$ ((1-x)BNT-xPT) solid solution and its composites with $Ni_{0.6}Zn_{0.4}Fe_2O_4$ including synthesis, crystal structures, dielectric properties, nature of phase transitions and magnetoelectric response of composite. Before starting discussion about important results of our investigations in subsequent chapters, we will briefly introduce the basic concepts/terms and the relevant ideas of magnetoelectric multiferroics in this chapter. Subsequently, we will present a brief review of existing literature on (1-x)$Bi(Ni_{1/2}Ti_{1/2})O_3$-x$PbTiO_3$ ((1-x)BNT-xPT) solid solution and composites of ferroelectrics with magnetic materials.

1.2 Perovskites Structure

Compounds with general formula ABO_3 having structure similar to that of $CaTiO_3$ may crystalline in perovskite structure. Perovskite name was taken from the perovskite mineral $CaTiO_3$ discovered in the Ural Mountain (Russia) by Gustav Rose (1839). Perovskite was named later by a Russian mineralogist L. A.

Perovski for the first time. Victor Goldschmidt described first the structure of perovskites in 1926 during his study on tolerance factors [Goldschmidt et al. (1926)]. The ideal perovskite-type (ABO_3) crystals belong to a cubic structure (space group $Pm\bar{3}m$) having A-site occupied by larger cation and B-site with a smaller cation. In the ideal cubic unit cell A-site ions occupy the corner position (0, 0, 0), B-site atoms at body centre position (1/2, 1/2, 1/2) and oxygen atoms at face centred positions (1/2, 1/2, 0). The A-site and B-site cations have 12-fold and 6-fold coordination, respectively, with the oxygen anions in ABO_3 perovskite unit cell. Fig.1.2 depicts the typical view of ABO_3 perovskite in which the centre position is occupied by the B cation. Ions are expected to touch each other in an ideal perovskite structure so that the B-O and A-O bonds following the relationship between the ionic radii as $(R_A + R_O) = \sqrt{2}\ (R_B + R_O)$. It has been found that this equation is not exactly followed in ABO_3 compounds while the XRD pattern reveals the cubic structure. Goldschmidt (1926) have defined a mathematical term called tolerance factor (t) to predict the deviation from ideal perovskite structure at room temperature which is defined in the equation (1.1)

$$t = \frac{(R_A + R_O)}{\sqrt{2}\ (R_B + R_O)} \quad \ldots\ldots\ldots\ldots\ldots\ldots \quad (1.1)$$

t=1, for ideal cubic perovskite structure. Cubic perovskite structure is also found for the tolerance factor in the range of $0.95 < t < 1.04$. A perovskite structure is stable if $0.80 < t < 1.1$. The 't' value is smaller than 1 if the size of 'A' atom is

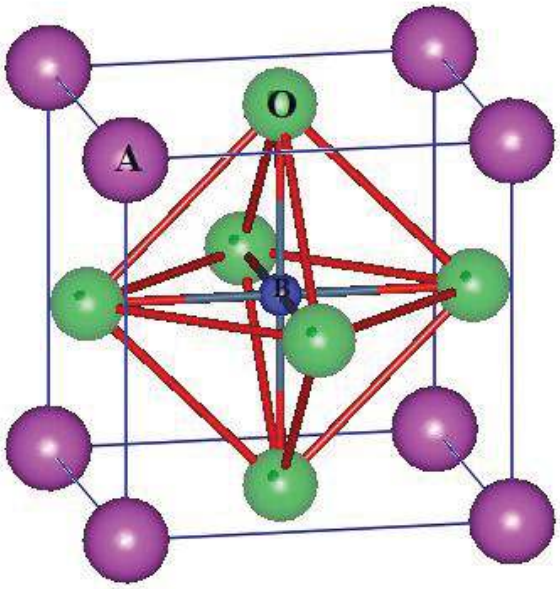

Fig.1.2. Ideal ABO_3 perovskite unit cell depicting 'A' ions at (0, 0, 0), the 'B' ion (1/2, 1/2, 1/2) and 'O' ions at (0, 1/2, 1/2) positions in cubic lattice.

smaller to occupy available volume which results into tilting of BO_6 octahedra. In case of $t > 1$, the B atom is too small and hexagonal structures with almost hexagonal close-packed layers of the A cations and O anions are formed. Thus, a tolerance factor < 1 suggests rotational instabilities. Compounds with $t > 1$ are known to exhibit ferroelectricity in the perovskite structure [Goldschmidt et al. (1926); Liang et al. (2004)].

1.3 Ferroelectricity and Anti-ferroelectricity

Ferroelectrics are the materials which possess spontaneous polarization and the direction of polarization can be switched hysterically by applying electric field [Jaffe et al. (1971); Lines and Glass (1977)]. Crystals are classified into 32 point groups. Out of these 32 point groups, 11 are centrosymmetric while 21 are non-centrosymmetric classes. Among these 21 non-centrosymmetric point groups, 20 (except 432) can show piezoelectric response. Positive and negative charges appear at the surface of these piezoelectric materials on application of stress. Out of 20 non-centrosymmetric point groups, the materials belonging from 10 point groups can show spontaneous polarization due to temperature change and are called pyroelectric. Ferroelectrics are those types of pyroelectric materials in which direction of spontaneous polarization can be reversed by applied electric field (within breakdown limit). The phenomenon of ferroelectricity was discovered in 1921 [Valasek (1921)]. The polarization-electric field (P-E) hysteresis for ferroelectric which exhibit a nonlinear hysteresis loop is shown in Fig.1.3. Ferroelectrics exhibit ferroelectricity only below a certain temperature known as Curie temperature (T_c).

(a)

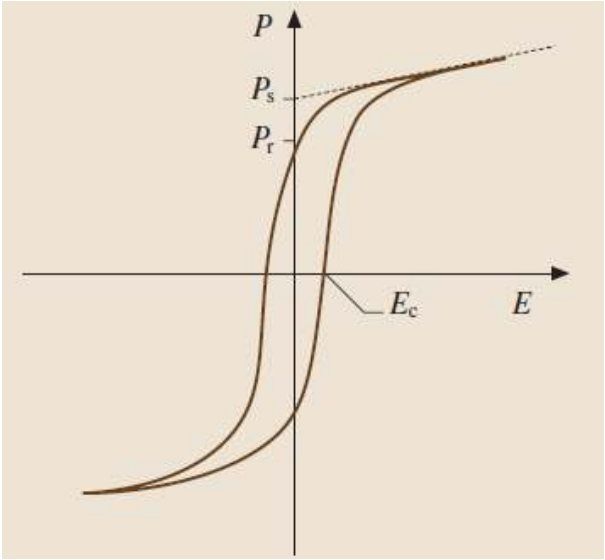

(b)

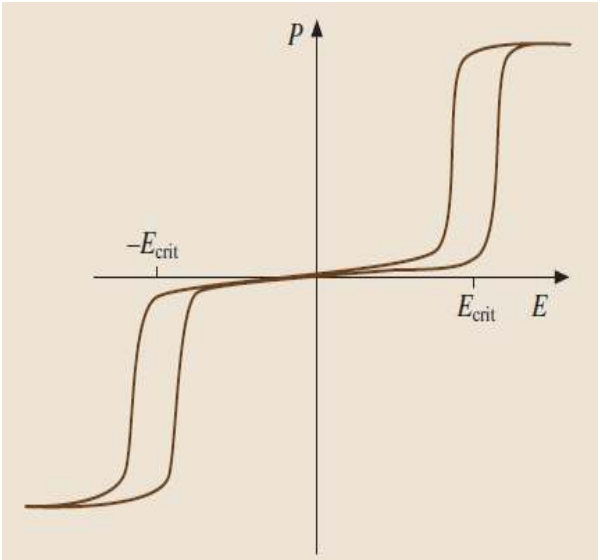

Fig.1.3. Polarization-electric field (P-E) hysteresis loop for (a) ferroelectric materials. (b) P-E hysteresis loop antiferroelectric materials [after Lines and Glass (1977); Uchino (2000); Martienssen et al. (2005)]

Above this temperature ferroelectrics behave as paraelectric and crystal structure become centrosymmetric cubic. Polarization switching has been described in detail for different ferroelectrics by Lines and Glass (1977). It has been proposed by Lines and Glass (1977) that domain structure in ferroelectrics is the key factor for the polarization switching. Polarization switching may occur by domain-wall motion, growth of existing antiparallel domains, nucleation and growth of new antiparallel domains [Lines and glass (1977)]. Application of electric field to ferroelectric material initially leads to the growth of domains in the direction of applied electric field. On further application of electric field, polarization increases non-linearly in the direction of electric field. At very high electric field polarization reaches to saturation (P_s) value. The material even retains remanent polarization (P_r) after reducing the applied electric field to zero. Polarization approaches to zero and display saturation polarization in the opposite direction on the reversal of applied electric field in the opposite direction. The field at which remanent polarization become zero is known as coercive field (E_c). Such types of materials undergo a phase transition from ferroelectric to paraelectric phase at Curie point (T_c). Dielectric constant ($\varepsilon^{/}$) for these materials follows the Curie-Weiss law [$\varepsilon^{/}=C/(T-T_o)$] where, C and T_o are Curie constant and Curie temperature, respectively. T_c is actual phase transition temperature which is found at higher temperature than T_o for first order phase transition but $T_c=T_o$ for second order phase transition [Lines and Glass (1977)].

Antiferroelectric materials consist of an ordered arrangement of dipoles but the adjacent dipoles are oriented in the opposite (anti-parallel) directions so that

total macroscopic spontaneous polarization is zero. Fig.1.3(b) shows the variation of electric polarization with applied electric field. At very low applied field, polarization is linearly proportional to the applied field. Application of the field above a critical level (E_t) transforms the crystal into ferroelectric phase so that it exhibit ferroelectric like loop. Crystal returns into initial state after the removal of the field with zero polarization. Similar phenomenon is observed by the reversal of electric field direction. Thus, antiferroelectric crystals exhibit double hysteresis loop [Kittel (1951); Uchino (1982)]. The transition temperature for antiferroelectric materials is commonly known as Neel temperature (T_N).

1.4 Relaxor-Ferroelectrics

Relaxor ferroelectrics are strongly disordered systems possessing peculiar structure and properties. Relaxors may exhibit giant dielectric and piezoelectric responses over a wide range of temperature [Bokov and Ye (2006); Smolensky (1981); Cross (1987); Viehland et al. (1992); Dmowski et al. (2008)]. Compositional disorder (also called chemical or ionic or substitutional disorder) is general characteristic of relaxors where equivalent crystallographic sites are occupied by different ions. For example in $Pb(Mg_{1/3}Nb_{2/3})O_3$ (PMN) [Smolenskii et al. (1961)], $Pb(Sc_{1/2}Ta_{1/2})O_3$ (PST) [Chu et al. (1993)], $Pb(Zn_{1/3}Nb_{2/3})O_3$ (PZN) [Bokov and Ye (2006)], $Pb(Mg_{1/3}Ta_{2/3})O_3$ [Bokov and Ye (2006)], $Pb(Sc_{1/2}Nb_{1/2})O_3$ [Bokov and Ye (2006)], $Pb(In_{0.5}Nb_{0.5})O_3$ [Bokov et al. (1999)] $(1-x)Pb(Mg_{1/3}Nb_{2/3})O_3$-$xPbTiO_3$ [Singh et al. (2006)], $(1-x)Pb(Zn_{1/3}Nb_{2/3})O_3$-$xPbTiO_3$ [Durbin et al. (1999)] and $(1-x)Bi(Mg_{1/2}Zr_{1/2})O_3$-$xPbTiO_3$ (BMZ-PT)

[Pandey et al. (2014)] 'B-sites' are occupied by non isovalent ions. Similar to the normal ferroelectrics, relaxors exist in a non-polar paraelectric (PE) state at high temperatures. They transform into the 'ergodic relaxor' state on lowering the temperature. This ergodic relaxor state contains the randomly distributed polar regions of nanometer scale (PNRs). Temperature at which transformation takes place is called as Burns temperature (T_B) [Bokov and Ye (2006)]. Such transformations are completely free from the structural modification. The PNRs (which are mobile near T_B) get frozen into a 'nonergodic state' at the temperature T_f (freezing temperature) on further cooling below T_B. However, the average symmetry of the crystal still remains unchanged and similar to that observed at high temperatures [Bokov and Ye (2006)]. Giant peak with wide frequency dispersion is observed in the temperature dependent dielectric permittivity (ε') due to freezing of PNRs. Depending upon the freezing of the PNR clusters, dielectric relaxation has been classified into two categories (i) Vogel-Fulcher type [Vogel (1921); Fulcher (1925)] and (ii) Arrhenius type [Bokov and Ye (2006); Singh et al. (2008)], as described in equations (1.2) and (1.3), respectively.

$$\tau = \tau_o \, e^{E_a/kT} \quad \ldots\ldots\ldots\ldots\ldots\ldots \quad (1.2)$$

$$\tau = \tau_o \, e^{E_a/k(T-T_{vf})} \quad \ldots\ldots\ldots\ldots\ldots \quad (1.3)$$

Where, E_a is the activation energy for thermally activated jump of polar clusters, τ_o is the relaxation time, *k* is Boltzmann constant and T_{vf} is Vogal-Fulcher freezing temperature. The phenomenon of relaxor ferroelectrics is still a matter of

debate as there is no satisfactory explanation for this behaviour. However, in recent years super-paraelectric [Cross (1994)], dipole glass [Viehland et al. (1991)], random field [Kleeman et al. (1997)] and random field-random bond [Blinc et al. (1999)] models have been proposed to understand this behaviour.

Fig.1.4(a) depicts the temperature-dependent dielectric measurements for BMZ-PT (x=0.56). Temperature variation of the permittivity exhibits large frequency dispersion and the peak temperatures in the real ($T_m^{/}$) and imaginary ($T_m^{//}$) parts of the permittivity do not coincide ($T_m^{//} < T_m^{/}$), suggesting the relaxor nature of phase transition. The permittivity peaks shift towards the higher temperature side on increasing the measuring frequency for both real and imaginary parts. All these features are basic characteristics of relaxor nature of phase transition. Fig.1.4(b) depicts the temperature dependence of the relaxation time (τ), as obtained from the $\varepsilon^{//}(T)$ data. The temperature-dependent relaxation time (τ) has been modeled using Arrhenius and Vogel-Fulcher type relations [Fu et al. (2009)]. The ln(τ) vs. 1/T fit is not linear for the Arrhenius plot. However, quite satisfactory linear fit is obtained for Vogel-Fulcher type relation with the activation energy (E_a)=2.3x10^{-3}eV, relaxation time (τ)=4.46x10^{-7}s with Vogel-Fulcher freezing temperature (T_{Vf}) of 482K [Pandey et al. (2014)]. The well-known example of such systems which follow Arrhenius relation is Li and Ti doped NiO [Wu et al. (2002)] and $BiFeO_3$-$BaTiO_3$ [Singh et al. (2008)].

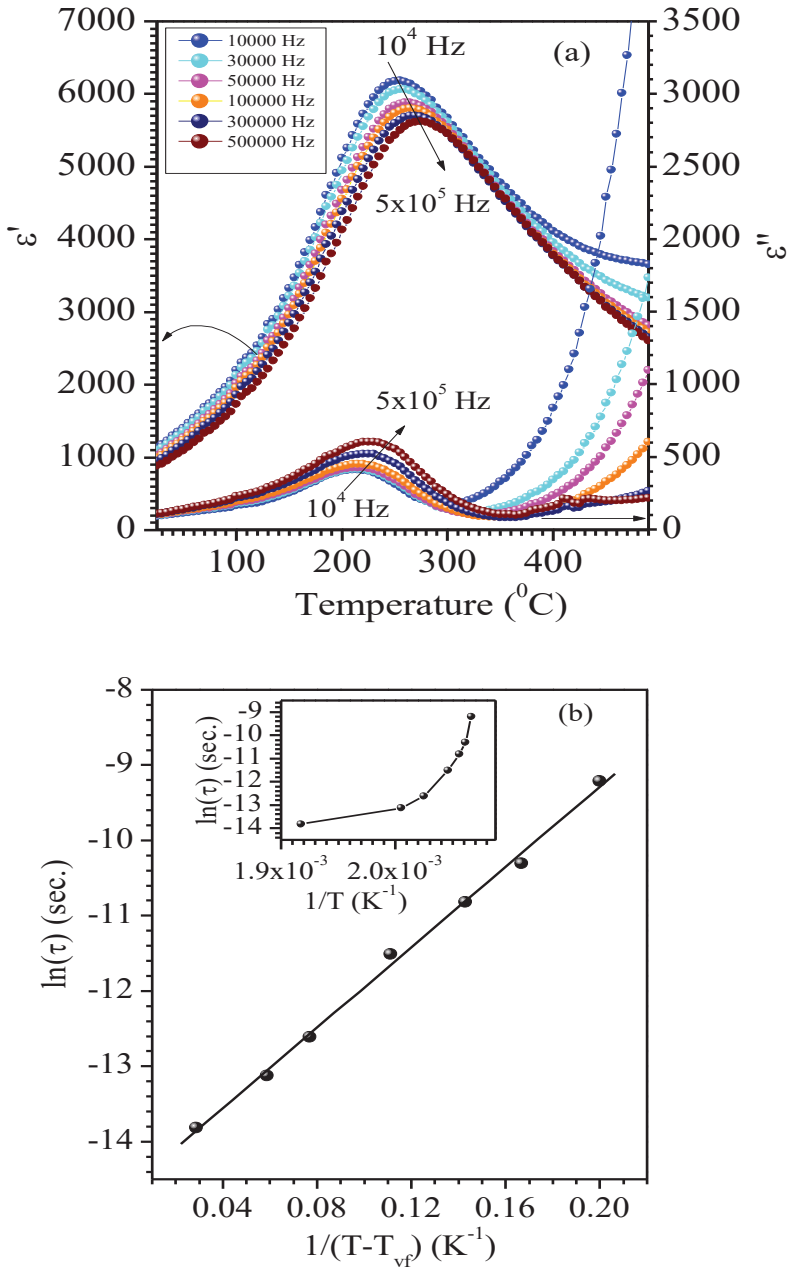

Fig.1.4. (a) Temperature variation of the real ($\varepsilon^{/}$) and imaginary ($\varepsilon^{//}$) parts of the permittivity for BMZ-PT with x=0.56 at various frequencies 10kHz, 30kHz, 50kHz, 100kHz, 300kHz and 500kHz. (b) Linear fit of the relaxation time (s) for the Vogel-Fulcher freezing. The inset shows the nonlinear nature of the ln(τ) vs. 1/T plot for the Arrhenius relationship [after Pandey et al. (2014)].

1.5 Ferromagnetism and Antiferromagnetism

Ferromagnetic materials possess spontaneous magnetization whose direction can be switched hysterically by applying external magnetic field. It is a quantum mechanical phenomenon originating from the exchange interaction. Existence of internal 'molecular field' favours the alignment the atomic moments parallel to each other in ferromagnetic materials [Cullity (1972)]. The spontaneous magnetization of ferromagnetic materials is stable only below a critical temperature called as Curie temperature (T_c). The material is ferromagnetic below the Curie temperature and becomes paramagnetic above this temperature. Above T_C the susceptibility (χ) varies according to the Curie-Weiss law given by $\chi=C/(T-T_c)$. Virgin samples of ferromagnetic materials contain magnetic domains oriented in different directions. The subsequent alignment and reorientation of the domains, upon the application of a magnetic field (H**)** is shown in Fig.1.4.(a). The domains change shape and size by the movement of domain boundaries on application of magnetic field. In the virgin sample of ferromagnetic materials, the moments of the constituent domains are initially randomly oriented so that there is no net magnetization (M). On application of the external field (H), the domains that are oriented in the favourable directions of the applied field grow in contrast to the domains of unfavourable orientations. The process continues with increasing field strength until the macroscopic specimen becomes a single domain. Saturation magnetization (M_s) is achieved when the orientation of this domain is along the direction of applied field H. The complete process of M-H hysteresis is shown in Fig.1.4(b) [Callister (2001)].

(a)

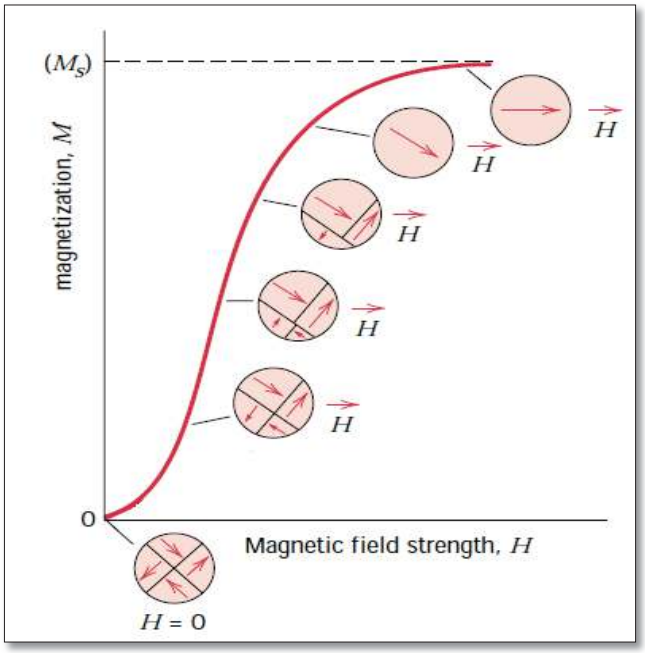

(b)

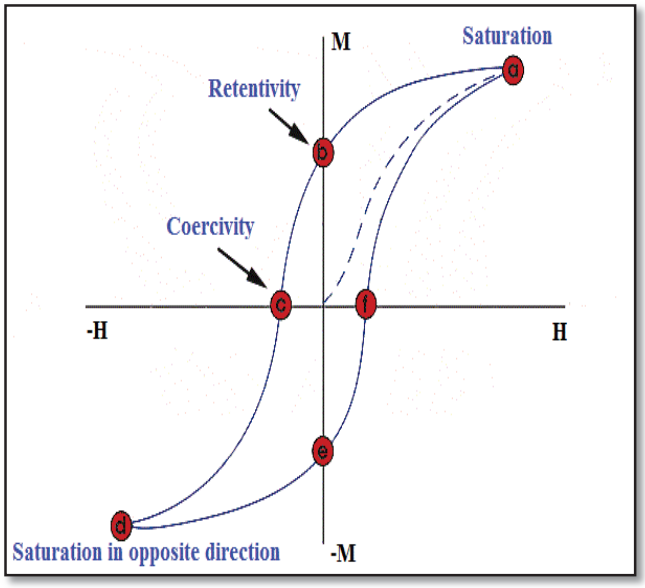

Fig.1.5. (a) Domain orientations at several stages of magnetization with applied field for ferromagnetic materials [after Wyatt and Hughes (1974); Callister (2001)]. (b) M-H hysteresis loop for ferromagnetic materials [from [https://www.nde-ed.org/Education Resources/CommunityCollege/MagParticle/Physics/HysteresisLoop.htm]

Still some net magnetization is present in the former direction even the applied field approaches to zero called as remanence magnetization (M_r). To reduce this magnetization to zero, negative magnetic field of strength ($-H_c$) will be needed which is known as coercivity. Saturation is ultimately achieved in the opposite direction with further increasing the negative field. In antiferromagnetic materials, spin moments of neighbouring atoms or ions align in exactly opposite directions. That is the reason one cannot expect the magnetization in the antiferromagnetic materials. Net magnetization is found in antiferromagnetic materials due to canted spin, defects in lattice and frustrated surface spins when the magnetic field is not present. Magnetization can be induced by applying sufficiently high external magnetic field due to the rotation of spin and spin flop. The antiferromagnetic character is observed at sufficiently low temperature called as 'Neel temperature' (T_N). Above the Neel temperature antiferromagnetic materials depict paramagnetic nature. Magnetic susceptibility (χ) increases, then display a maximum at T_N and further decreases as the temperature is lowered below T_N. Antiparallel alignment of moments is strong enough which act even applied field is not present due to insignificant thermal randomization [Kittel (1977); Callister (2001)].

1.6 Magnetoelectric Coupling in Single Phase Multiferroics

The magnetoelectric (ME) effect in single phase multiferroics may be defined as the coupling between electric and magnetic order parameter where magnetization (M) can be produced by applying an electric field (E) and vice-versa [Fiebig (2005)]. Magnetoelectric effect in single phase multiferroics is

thermodynamically described in the framework of Landau theory of free energy. The expression of free energy 'F' of the multiferroic system is written in equation (1.4) in the terms of an applied magnetic field 'H' whose i-th component is H_i and an applied electric field 'E' whose i-th component is E_i, F_o denotes the ground state free energy of the system [Fiebig (2005); Wang et al. (2009); Eerenstein et al. (2006)].

$$F(E, H)=F_0- P^s_iE_i- M^s_iH_i- 1/2\varepsilon_0\varepsilon_{ij}E_iE_j- 1/2\mu_0\mu_{ij}H_iH_j- \alpha_{ij}E_iH_j- 1/2\beta_{ijk}E_iH_jH_k$$
$$-1/2\gamma_{ijk}H_iE_jE_k - \ldots\ldots\ldots\ldots\ldots\ldots\ldots\ldots \quad (1.4)$$

Where, subscripts (i, j, k) refer to the three components of the electric field E (E_i, E_j, E_k) and magnetic field H (H_i, H_j, H_k). P^s_i and M^s_i refer to the components of spontaneous polarization P^s and magnetization M^s, ε_0 and μ_0 are the dielectric permittivity and magnetic permeability of vacuum respectively, ε_{ij} the electric permittivity and μ_{ij} the magnetic permeability. The second rank tensor α_{ij} denotes the induction of polarization by a magnetic field or of magnetization by an electric field which is named as the linear magnetoelectric coefficient. The third rank tensors β_{ijk} and γ_{ijk} represent higher order magnetoelectric coefficients. The magnetoelectric effects can then be easily expressed in the form $P_i(H_i)$ and $M_i(E_i)$ by differentiating equation (1.4) w.r.t. E_i and H_i and then setting E_i and H_i =0.

$$P_i(E, H)=- \partial F/\partial E_i= P^s_i+ \varepsilon_0\varepsilon_{ij}E_j+ \alpha_{ij}H_j+ \beta_{ijk}H_jH_k+ \gamma_{ijk}H_iE_j\ldots\ldots\ldots(1.5)$$

$$M_i(E, H) = -\partial F/\partial H_i = M^s{}_i + \mu_0\mu_{ij}H_j + \alpha_{ij}E_j + \beta_{ijk}H_jE_i + 1/2\gamma_{ijk}E_jE_k \ldots (1.6)$$

However, the magnetoelectric effect in single-phase multiferroics is generally too small to be useful for device applications. Giant magnetoelectric effect is reported to appear in composite materials [Fiebig (2005); Nan et al. (2008); Zeng et al. (2004); Dong et al. (2003)].

1.7 Conflicting Requirements for Ferroelectricity and Ferromagnetism in Single Phase Materials

Theoretical studies on ferroelectricity and magnetism reveal that coexistence of ferroelectricity and magnetism in single phase material is a challenging task. First principles [Cohen and Krakauer (1992)] density functional theory (DFT) within the local density approximation (LDA) suggests that the hybridization between Ti '3d' and O '2p' orbitals is essential for stabilizing the ferroelectric distortion in $PbTiO_3$ and $BaTiO_3$. Ti^{4+} ion is present in d^0-state in these ferroelectrics. The lowest unoccupied energy levels are d-states which favours the hybridization with O '2p' state. In contrast, unpaired electrons in the d-orbital (d^n) at B-site cations is an essential requirement for the existence of magnetic moments and thus magnetic ordering.

To resolve this contradictory requirement, attempt was done by Russian scientist by putting both d^0 (ferroelectrically active) and d^n (magnetically active) cations at B-site of perovskite materials. Following this scheme multiferroic systems such as $Pb(Fe_{1/2}Nb_{1/2})O_3$ (PFN), $Pb(Fe_{2/3}W_{1/3})O_3$ (PFW),

$Pb(Ni_{1/3}Nb_{2/3})O_3$ (PNN) etc were synthesized containing Nb^{5+} and W^{+6} as ferroelectrically active ions while Fe^{3+} and Ni^{2+} as magnetically active ions. [Fiebig (2005); Wang et al. (2009); Smolenskii and Agranovskaya (1958)] However, these materials exhibit magnetoelectric coupling well below the room temperature which is not suitable for application at room temperature.

1.8 Multiferroic Character in Single Phase d^n-Systems

In order to get the ferroelectricity in perovskites, requirement of d^0-ness for B-site cation is proposed to be an essential condition. However, appearance of ferroelectricity is also reported in many single phase materials which contain d^n electrons such as $BiFeO_3$ [Jacobson and Fender (1975); Kaczmarek and Pajak (1975); Pradhan et al. (2005)], $BiMnO_3$ [Seshadri and Hill (2001); Atou et al. (1999)] etc. Presence of unpaired electrons in the d-orbital of B-site cations results in magnetism but the d^0-ness requirement for ferroelectricity is violated. To explain the presence of ferroelectricity in d^n systems, different mechanisms have been proposed which are grouped primarily in four different categories as discussed below [Ramesh and Spaldin (2007); Cheong and Mostovoy (2007); Eerenstein et al. (2006)].

1.8.1 Ferroelectricity Induced by Lone Pair of Electrons

This type of ferroelectricity is found in the multiferroics containing the lone-pair of electrons in s-orbit of the A-site cation. For example, in $BiFeO_3$ or $BiMnO_3$ lone-pair of electrons in 6s orbit of Bi^{3+} ion move away from the centrosymmetric position of surrounding oxygen and results in ferroelectricity [Wang et al. (2009)]. Since the lone-pair state is chemically unstable and allow

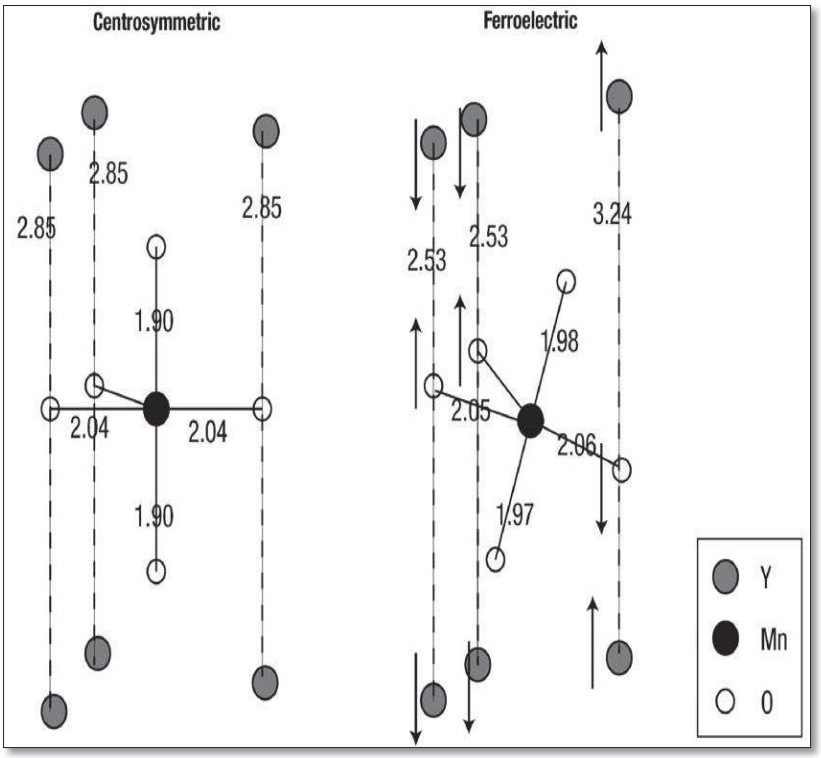

Fig.1.6. Crystal structure of $YMnO_3$ in centrosymmetric paraelectric phase. Buckling of MnO_5 pyramid in the ferroelectric phase of $YMnO_3$ with arrows indicating the position of atoms with respect to the centrosymmetric paraelectric phase. [after Aken et al. (2004)].

the mixing between the ground state $(ns)^2$ and a low-lying $(ns)^1(np)^1$ excited state. This leads to the breaking of inversion symmetry and turns into ferroelectricity [Trinquier and Hoffmann (1984); Waston et al. (1999); Seshadri and Hill (2001)]. It is well-known that magnetism appears due to magnetic ions Fe^{3+} and Mn^{3+} ions in such multiferroics. Materials in which ferroelectricity originates from the lone-pair effect are called as 'proper ferroelectrics'. Other type of materials in which ferroelectricity induces from the lattice distortion are known as 'improper ferroelectrics'.

1.8.2 Ferroelectricity Induced by Geometric Frustration

Ferroelectricity induced by geometrical frustration is observed generally in hexagonal manganites ($RMnO_3$, R: rare earth elements). For example, the hexagonal manganites $YMnO_3$ consist of non-connected layers of MnO_5 trigonal bipyramids with corner linked by inplane oxygen (O_p) and apical oxygen ions (O_T) forming close-packed planes separated by a layer of Y^{3+} ions. Due to the layered structure and the triangular symmetry, buckling of MnO_5 trigonal bipyramids (in order to reach the close packing) breaks the inversion symmetry and results the ferroelectric state. This turns into shorter c-axis and two longer Y-O_P bonds as shown in Fig.1.6. Further, Y-ions vertically shift away from the centrosymmetric position. Therefore, one of the two Y-O_P (2.8Å) bond length is reduced down to (2.3Å) and the other is elongated to (3.4Å) leading to a net electric polarization. The dipole moments mostly formed by Y-O pairs and not from Mn-O pairs [Aken et al. (2004)] as shown in Fig.1.6. Thus, ferroelectricity is again driven by A-site cation in $YMnO_3$ where the d^0-ness rule is violated.

1.8.3 Ferroelectricity in Charge Ordered Multiferroics

In charge ordered multiferroics, certain 'non-centrosymmetric' arrangements of ions induce ferroelectricity in magnetic materials [Ramesh (2009)]. In the charge ordered systems, magnetic ion possesses the variable valence state. Charge ordering was at first investigated in $LuFe_2O_4$ [Cheong and Mostovoy (2007); Wang et al. (2009)]. The charge ordered pattern of $LuFe_2O_4$ contains alternating Fe^{2+} and Fe^{3+} layers at 370K. Charge ordered structure produces the local electric polarization due the non- coincidence of Fe^{2+} and Fe^{3+} ions centre [Cheong and Mostovoy (2007)].

1.8.4 Ferroelectricity due to Spiral-Spin Ordering

It has been observed that some materials exhibit ferroelectricity which is directly induced by the spin ordering. The induced electric polarization (**P**) is directly proportional to the vector product of spin (**e**) and wave vector of a spiral (**Q**) in spin-ordered multiferroics [Cheong et al. (2007); Mostovoy (2006), Singh (2012)]

$$\mathbf{P} \propto \mathbf{e} \times \mathbf{Q} \quad \ldots\ldots\ldots\ldots\ldots\ldots \quad (1.7)$$

Such type of multiferroic character is found in $RMnO_3$ (R=Tb, Gd) [Cheong et al. (2007)].

1.9 $Bi(Ni_{1/2}Ti_{1/2})O_3$ as a Multiferroic System

$Bi(Ni_{1/2}Ti_{1/2})O_3$ (BNT) is newly synthesized multiferroic material. The first study of BNT as a multiferroic material was carried out by Zhu et al [Zhu et al. (2013)]. BNT reveals a paraelectric to ferroelectric phase transition at 240^0C. The magnetic structure of BNT is very complex. At the applied magnetic field of

lower strength, BNT exhibits an antiferromagnetic transition around 58K. On increasing the field strength up to 7T, it shows a ferromagnetic like phase transition [Zhu et al. (2013)]. However, BNT cannot be synthesized at ambient pressure and high sintering temperature due to its lower tolerance factor t=0.888 [Inaguma and Katsumata (2003); Zhu et al. 2013]. It requires high pressure (5-6GPa) as well as high temperature (1000^0C) for synthesizing in phase pure perovskite state [Inaguma and Katsumata (2003); Zhu et al, 2013]. Not only in BNT, high pressure synthesis is also required in other Bi-based perovskite systems such as $Bi(Zn_{1/2}Ti_{1/2})O_3$ (BZT), $Bi(Mg_{1/2}Zr_{1/2})O_3$, $Bi(Mg_{1/2}Ti_{1/2})O_3$, and Bi_2MnNiO_6 [Pandey et al. (2013); Pandey et al. (2014); Sharma et al. (2013); Suchomel et al. (2006); Khalyavin et al. (2006); Azuma et al. (2005)].

1.10 Room Temperature Structure of Multiferroic $Bi(Ni_{1/2}Ti_{1/2})O_3$

As discussed above, BNT cannot synthesized at ambient pressure by using conventional solid state ceramic route. Powder XRD pattern of BNT sintered at 1000^0C (but at ambient pressure) reveals several impurity phases of $Bi_4Ti_3O_{12}$, NiO and Bi_2O_3 [Okuda et al. (1999)]. BNT synthesized under high pressure ~ (5-6)GPa (at 1000^0C) get stabilized in the double perovskite structure with space group $Pn2_1a$ [Zhu et al. (2013)]. Rietveld fit for $2Bi(Ni_{1/2}Ti_{1/2})O_3$ [can be also written as Bi_2NiTiO_6] synthesized at high pressure with simulated crystal structure is shown in Fig.1.7. The refined lattice parameters are reported to be a=5.61(1)Å, b=7.85(1)Å and c=5.58(1)Å [Zhu et al. (2013)]. Two isostructural phase transitions at 2GPa and 15GPa were observed in Bi_2NiTiO_6 at high

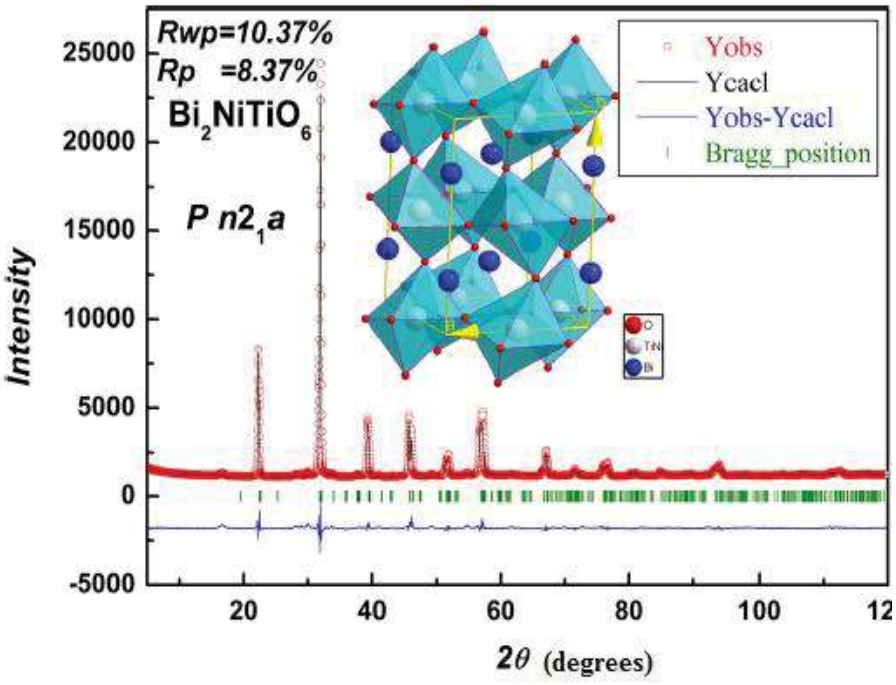

Fig.1.7. Observed (red dot), calculated (solid line) and difference (solid blue line) obtained by Rietveld analysis of the powder X-ray diffraction data of Bi_2NiTiO_6 at room temperature. Vertical tick-marks show the peaks positions. Crystal structure corresponds to orthorhombic in the space group $Pn2_1a$ of Bi_2NiTiO_6 [after Zhu et al. (2013)].

pressure and room temperature. Similar type of phase transition is also observed around the temperature higher than 550^0C at ambient pressure. This iso-structural phase transition is expected to occur due to sifting of Bi-ions from their Wyckoff position [Zhu et al. (2013)].

1.11 Multiferroic Properties of $Bi(Ni_{1/2}Ti_{1/2})O_3$

As discussed above, BNT is a multiferroic material and hence exhibits both ferroelectric and magnetic properties. Dielectric behaviour of BNT synthesized at high pressure is shown in Fig.1.8(a). Hysteresis for heating and cooling cycles of permittivity signifies the first order ferroelectric phase transition in BNT around 240^0C [Zhu et al. (2013)]. Zero field cooled (ZFC) and field cooled (FC) magnetic susceptibility (χ) of BNT measured at 100Oe is shown in Fig.1.8(b). Magnetic susceptibility (χ) of BNT reflects strong antiferroelectric nature around 58K. BNT demonstrates a ferromagnetic-like behaviour on increasing the field strength upto 7T [Zhu et al. (2013)]. Thus, presence of both ferroelectricity and magnetism makes BNT a multiferroic system below 58K. Linear part (inset Fig.1.7(b)) of inverse of magnetic susceptibility ($1/\chi$), fitted by Curie-Weiss law according to $1/\chi=(T+T_\theta)/C$ results in to T_θ=-242.7K and effective magnetic moment $\mu_{eff.}$=2.28 μB/f.u. depicts a strong antiferromagnetic and magnetic frustration in BNT [Zhu et al. (2013)].

1.12 Solid Solution of $Bi(Ni_{1/2}Ti_{1/2})O_3$ with other Perovskites

As discussed above, synthesis of phase pure BNT at ambient conditions is a tuff work due to its low tolerance factor (0.888) [Inaguma et al. (2003)].

(a)

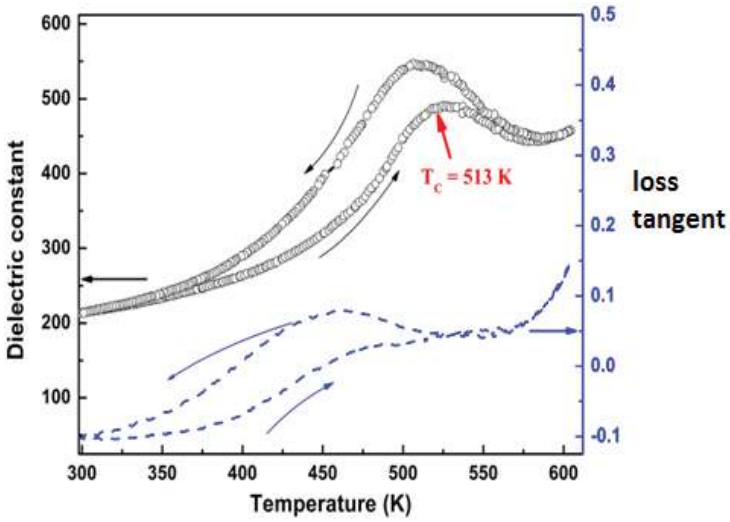

(b)

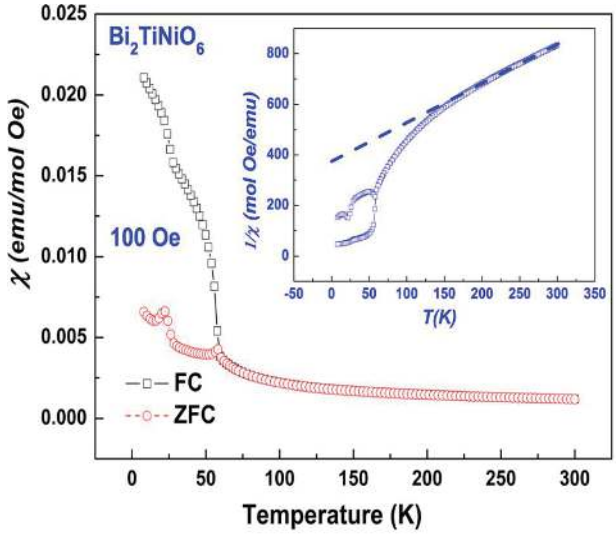

Fig.1.8. (a) Temperature variation of dielectric constant and dielectric loss (tanδ) at 100 kHz for $2Bi(Ni_{1/2}Ti_{1/2})O_3$ at room temperature. (b) ZFC and FC magnetic susceptibilities of $2Bi(Ni_{1/2}Ti_{1/2})O_3$ measured at the magnetic field strength of 100Oe. Inset shows the inverse of susceptibility at ZFC and FC [after Zhu et al. (2013)].

Formation of solid solutions with other stable perovskites such as $PbTiO_3$, $BaTiO_3$, etc may be other approach to form the phase pure solid solution of BNT at ambient pressure. The crystal and magnetic structures of the resultant system may be different from the initial component after the formation of solid solution. Phase pure perovskite form of BNT has been stabilized at ambient pressure by forming its solid solution with other ceramics such as $PbTiO_3$ [Choi et al. (2005)], $Pb_{(1-x)}Sr_xTiO_3$ [Kang et al. (2012)], $(K_{0.5}Bi_{0.5})TiO_3$ [Zhao and Zuo (2013)] etc. As discussed above, the structure of BNT is double perovskite with orthorhombic space group $Pn2_1a$ obtained by the repetition of monoclinic unit cells [Zhu et al. (2013)]. However, the room temperature structure of BNT entirely changes after solid solution formation with other ceramics. A Lead-free solid solution $(1-x)(K_{0.5}Bi_{0.5})TiO_3$-$xBi(Ni_{1/2}Ti_{1/2})O_3$ [Zhao and Zuo (2013)] formed by conventional solid-state route is reported to exhibit a phase transition from rhombohedral to tetragonal phase in the composition range of x=0.05-0.07. Impurity phase of $K_4Ti_3O_8$ appear with x>0.20 due to lower solubility of BNT in the $(K_{0.5}Bi_{0.5})TiO_3$ and smaller tolerance factor of BNT [Zhao and Zuo (2013)]. Powder XRD pattern of $(1-x)(K_{0.5}Bi_{0.5})TiO_3$-$xBi(Ni_{1/2}Ti_{1/2})O_3$ solid solution synthesized at room temperature is shown in Fig.1.9. Solid solution $(1-x)Bi(Ni_{1/2}Ti_{1/2})O_3$-$x(Pb_{(1-y)}Sr_yTiO_3)$ (BNT-PST) is also synthesized by solid state route aiming to reduce the leakage current by partial substitution of Sr at the place of Pb [Kang et al. (2012)]. Phase transition from the tetragonal phase to the rhombohedral phase is observed for this solid solution. The MPB region is determined in the vicinity of $0.45<x<0.47$. Similar type of phase transition is

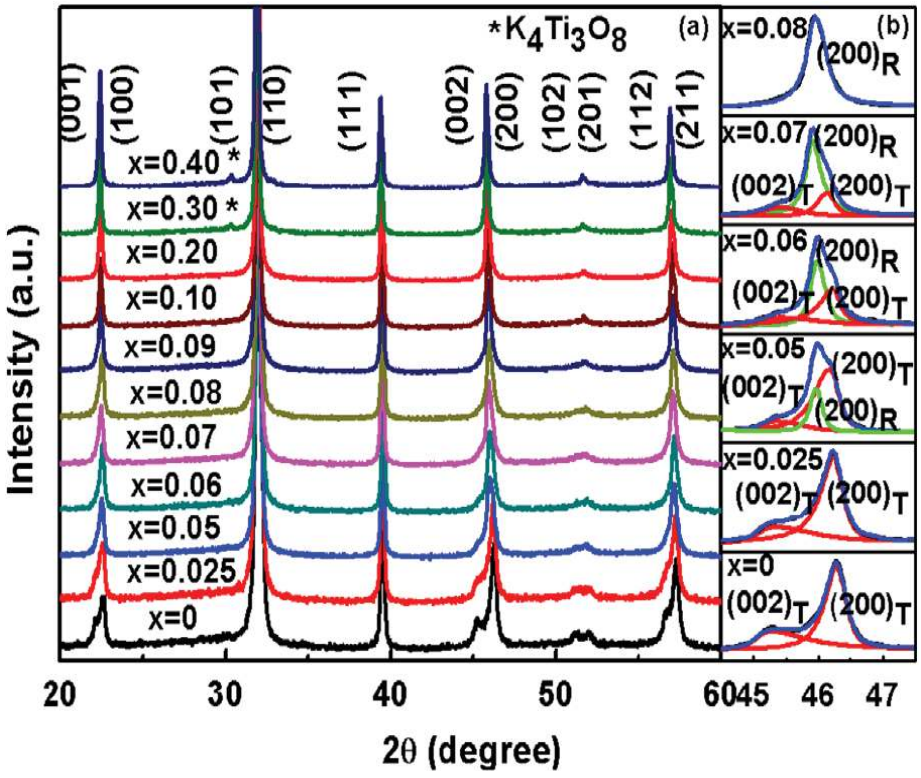

Fig.1.9. Powder XRD pattern of (1-x)($K_{0.5}Bi_{0.5}$)TiO_3-xBi($Ni_{1/2}Ti_{1/2}$)O_3 solid solution at room temperature for various compositions. Asterisk corresponds to the impurity phases $K_4Ti_3O_8$ [after Zhao and Zuo (2013)].

observed in the (1-x)$Bi(Ni_{1/2}Ti_{1/2})O_3$-x$(Pb_{0.9}Sr_{0.1}TiO_3)$ solid solution with shift in the MPB in the range of $0.47<x<0.51$ [Kang et al. (2012)]. Partial substitution of 'Pb' by 'Ba' in (1-x)$Bi(Ni_{1/2}Ti_{1/2})O_3$-x$(Pb_aBa_bTiO_3)$ (a+b=1) solid solution depicts either the presence of impurity phases or phase pure cubic structure with absence of MPB region.

1.13 Morphotropic Phase Boundary in Ferroelectric Solid Solutions

Morphotropic phase boundary (MPB) is a nearly vertical phase boundary between temperature-composition phase diagram of ferroelectric solid solution separating stability region of two crystallographic phases [Ahart et al. (2008)]. MPB exists around a particular compositional region where an abrupt change in the crystal structure of the solid solutions take place which results into maximization of physical properties. It was defined first for the $Pb(Zr_xTi_{1-x})O_3$ ($PbZrO_3$+$PbTiO_3$) solid solution separating the stability region of tetragonal and rhombohedral phases. Before starting a discussion on MPB in BNT-PT solid solution, it will be interesting to have a brief overview of MPB in well-known and widely used piezoceramic $Pb(Zr_xTi_{1-x})O_3$ (PZT).

Jaffe et al. (1971) first reported the MPB in PZT as shown in Fig.1.10(a) and proposed that it separates the phase boundary between rhombohedral and tetragonal phases with the coexistence of these two phases in the vicinity of MPB composition x=0.48. Fig.1.10(b) shows the composition dependence of dielectric permittivity ($\varepsilon^{/}$) and electromechanical coupling coefficient (k_P) which are maximized around the MPB composition x=0.48 [Jaffe et al. (1971)].

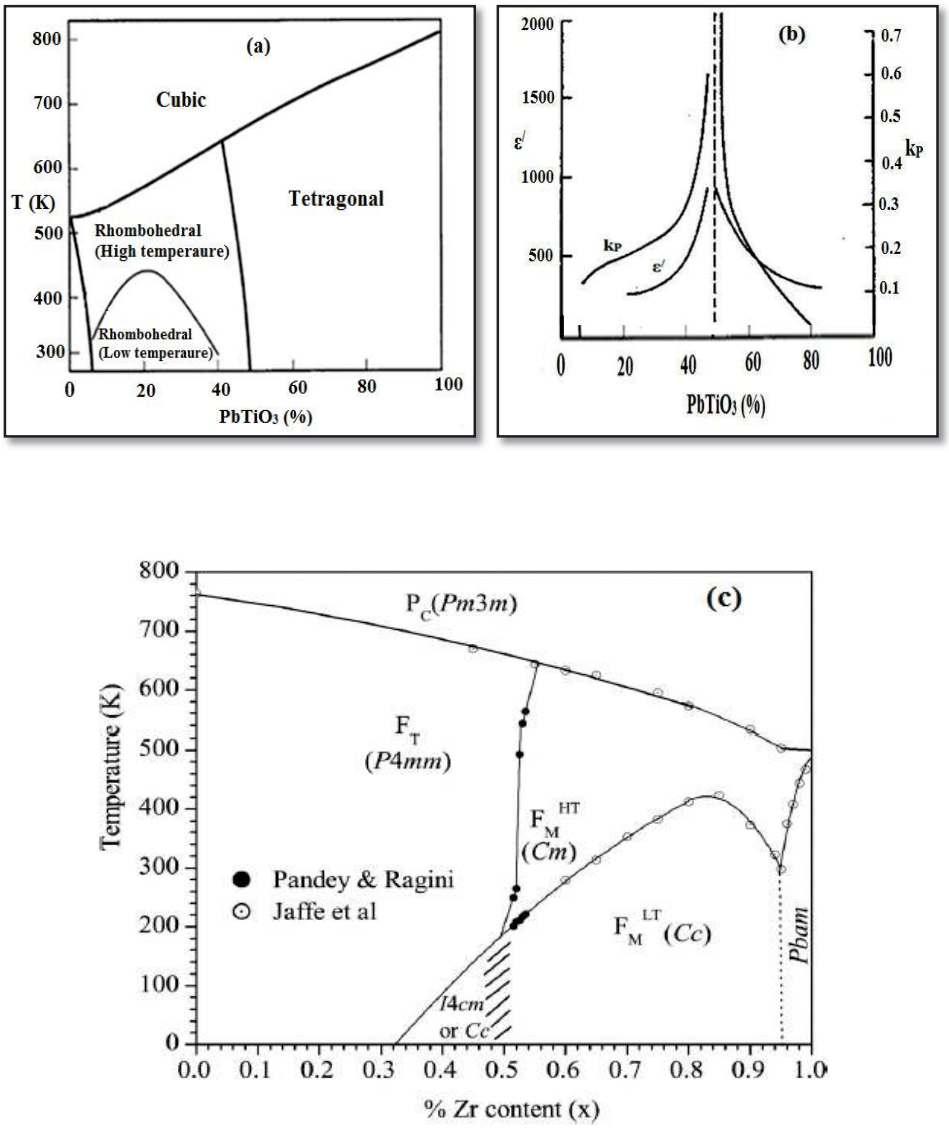

Fig.1.10. (a) Phase diagram for PZT [after Jaffe et al. (1971)] (b) Permittivity ($\varepsilon^{/}$) and planer electromechanical coupling coefficient (k_p) for PZT [after Jaffe et al. (1971)] (c) New phase diagram for PZT [after Pandey et al. (2008)].

Fig.1.10(a) shows the old phase diagram of PZT. In recent years, new monoclinic phases Cm and Cc were investigated in the MPB region of PZT [Noheda et al. (1999); Pandey et al. (2008)]. There is no satisfactory explanation for the maximization of physical properties in the vicinity of MPB till now. However, three different models [Pandey et al. (2008)] based on phase coexistence [Isupov (1968)], lattice instability [Mishra et al. (1996)] and polarization rotation [Fu and Cohen (2000)] have been proposed to explain this behaviour. In recent years, monoclinic phases have been discovered in the MPB region of several other solid solutions having high piezoelectric response like (1-x)$Pb(Mg_{1/3}Nb_{2/3})O_3$-x$PbTiO_3$ [Singh et al. (2006)], (1-x)$Pb(Zn_{1/3}Nb_{2/3})O_3$-x$PbTiO_3$ [Durbin et al. (1999)], (1-x)$Pb(Fe_{1/3}Nb_{2/3})O_3$-x$PbTiO_3$ [Singh et al. (2008)] .

1.14 Solid Solution of $Bi(Ni_{1/2}Ti_{1/2})O_3$ with $PbTiO_3$

Recently, several papers have been published on the solid solution of BNT with $PbTiO_3$ due to its high piezoelectric response and multiferroic character [Pandey et al (2014); Hu et al (2010); Choi et al. (2005). Kang et al. (2012); Zhang et al. (2012); Xie et al. (2013); Jianga et al. (2014); Kang et al. (2013); Wu et al. (2011)]. Zhang et al. have reported the presence of MPB in the composition range 0.46-0.48 (as shown in Fig.1.11) similar to well-known piezoceramic PZT. Choi et al. (2005) have reported the phase diagram of BNT-PT using the results of calorimetric and dielectric studies without systematic structural studies. Kang et al. [Kang et al. (2013)] have shown that the structure of BNT-PT across MPB is affected by the compositional fluctuations also.

Modification of the crystal structure of BNT-PT is observed by the addition of excess amount of PbO, NiO, TiO_2 and Bi_2O_3 during synthesis. Doping of 1 to 3 mole % of PbO, NiO and Bi_2O_3 transforms the MPB phase into tetragonal phase but the effect is less prominent after the doping of 1-5 mole % TiO_2. BNT-PT based ternary systems, such as (1-x-y)$PbTiO_3$-x$Bi(Ni_{1/2}Ti_{1/2})O_3$-y$BiScO_3$ [Hu et al. (2012)], (1-x-y)$PbTiO_3$-x$Bi(Ni_{1/2}Ti_{1/2})O_3$-y$BiFeO_3$ [Hu et al. (2011)] and $PbTiO_3$-$Bi(Ni_{1/2}Ti_{1/2})O_3$-$PbZrO_3$ [Kang et al. (2013)] have been reported with excellent ferroelectric and magnetic properties.

1.15 Phase Diagram of (1-x)$Bi(Ni_{1/2}Ti_{1/2})O_3$-x$PbTiO_3$

The phase diagram (Fig1.12(a)) of (1-x)$Bi(Ni_{1/2}Ti_{1/2})O_3$-x$PbTiO_3$ solid solution was at first reported by Choi et al [Choi et al. (2005)] using dielectric and calorimetric data. $PbTiO_3$ has tetragonal (c/a=1.06) structure at room temperature [Jaffe et al. (1971)] and exhibits a first-order phase transition at 495^0C. After the solid solution formation of BNT with $PbTiO_3$ the paraelectric-ferroelectric transition temperature increases up to 503^0C for a 0.1BNT-0.9PT composition [Choi et al. (2005)]. It has been proposed that the enhancement in transition temperature is linked with the random-field effect [Stephanovich et al. (2004); Stringer et al. (2006)]. For higher concentration of BNT in BNT-PT solid solution the transition temperature decreases systematically approaches to 400^0C around the MPB. The phase coexistence region is reported around x=0.49. Fig.1.12(b) depicts the variation of lattice parameter with increasing BNT concentration. Structural phase transition from tetragonal to pseudocubic phase is

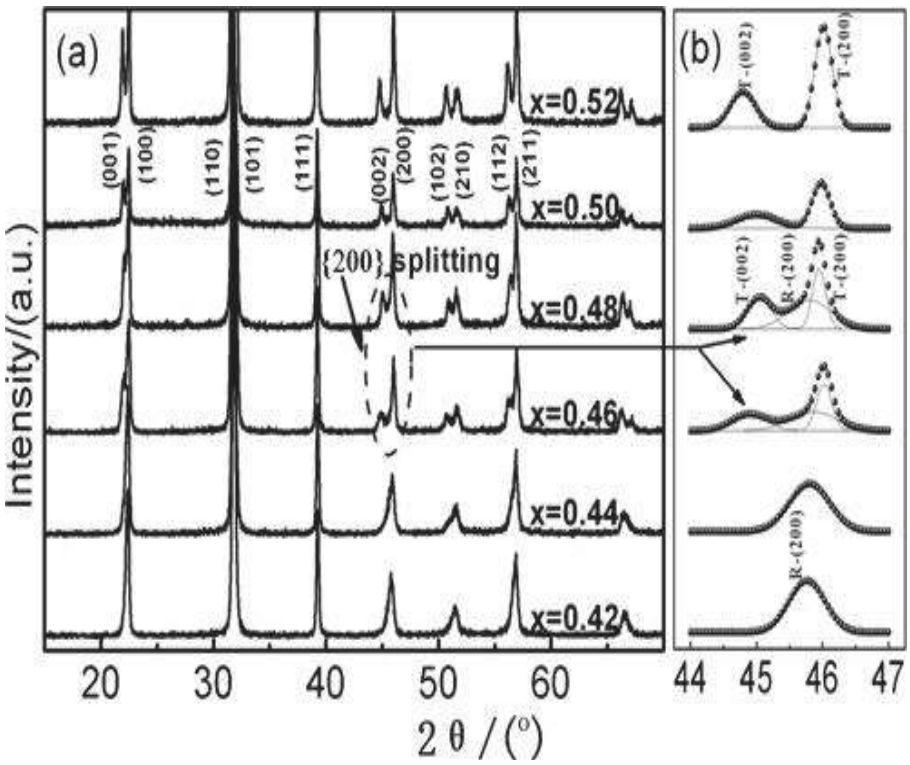

Fig.1.11. (a) Powder XRD pattern of (1-x)Bi($Ni_{1/2}Ti_{1/2}$)O_3-x$PbTiO_3$ solid solution in the composition range x=0.42-0.52. (b) (200) pseudocubic reflections of (1-x)Bi($Ni_{1/2}Ti_{1/2}$)O_3-x$PbTiO_3$ solid solution [after Zhang et al. (2012)].

reported for the higher concentration of BNT for the composition with x=0.48 [Hu et al. (2010)].

1.16 Multiferroic Character of (1-x)$Bi(Ni_{1/2}Ti_{1/2})O_3$-x$PbTiO_3$

In the present thesis work, we have chosen the solid solution of $Bi(Ni_{1/2}Ti_{1/2})O_3$ (BNT) with $PbTiO_3$ (PT) [i.e. (1-x)$Bi(Ni_{1/2}Ti_{1/2})O_3$-x$PbTiO_3$] for study. The solid solution (1-x)$Bi(Ni_{1/2}Ti_{1/2})O_3$-x$PbTiO_3$ is reported to be a multiferroic material with both ferroelectric and magnetic ordering [Hu et al. (2010)]. Polarization-electric field (P-E) hysteresis exhibits a coercive field $E_c \sim$ 38kV/cm at room temperature as shown in Fig.1.13(a). Maximum $d_{33} \sim$ 260pC/N is found for the composition with x=0.49 (Fig.1.13(b)). The shape of P-E hysteresis loop depicts the lossy character of sample at larger electric fields. Addition of 0.3 wt % of MnO_2 after calcination remove the problem a leakage current but leads to diminished polarization [Choi et al. (2005)].

M-H hysteresis of BNT-PT is shown in Fig.1.13(c). The magnetic structure of BNT-PT completely differs from BNT and shows ferromagnetic behaviour. Hu et al. (2010) have proposed that the ferromagnetism is linked with the superexchange interaction in BNT-PT solid solution [Hu et al. (2010)]. Large concentration of BNT reduces the ferromagnetic nature due to the increasing 'a' cell parameter of the tetragonal unit cell which weakens the super-exchange interaction [Hu et al. (2010)]. Ferromagnetic nature also reduces with increasing temperature due to the elongation of 'a' cell parameter of tetragonal unit cell.

However two drawbacks, (i) very low value of magnetoelectric (ME) coefficient and (ii) ME response below room temperature, make these single

(a)

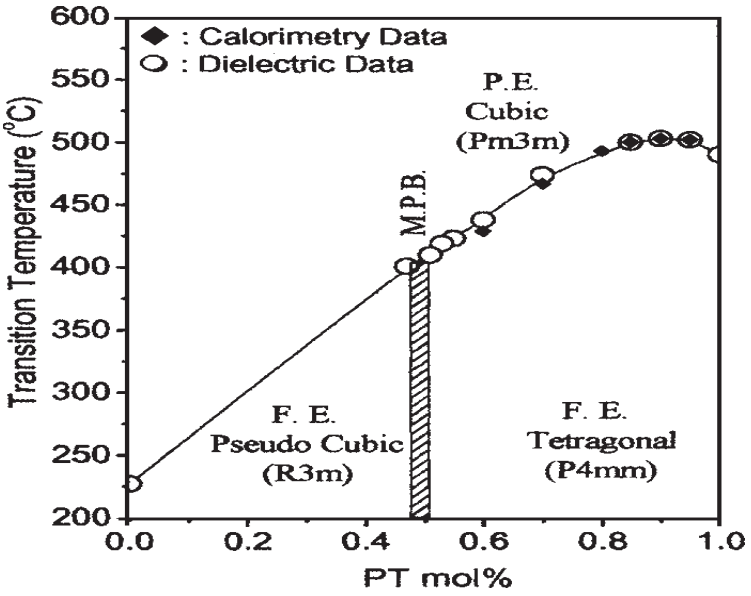

(b)

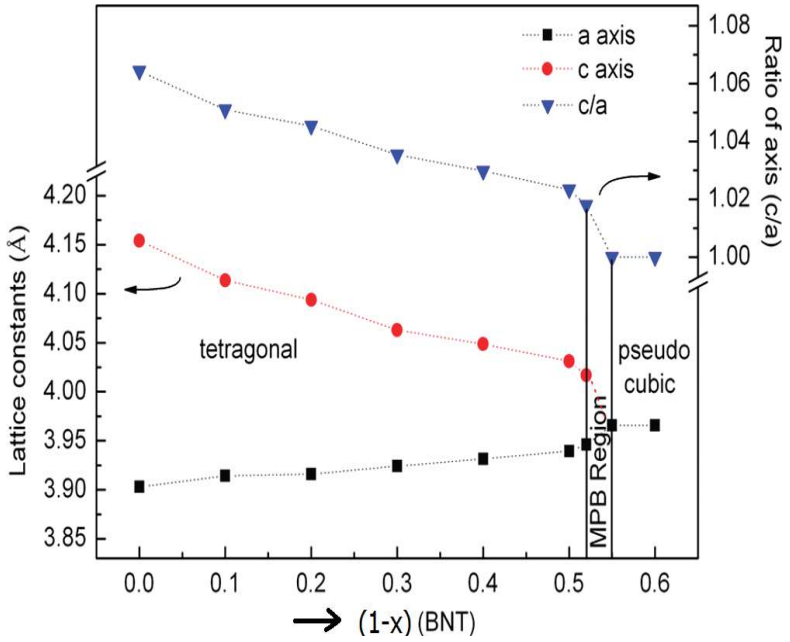

Fig.1.12 (a) Phase diagram of (1-x)Bi($Ni_{1/2}Ti_{1/2}$)O_3-x$PbTiO_3$ solid solution using calorimetric and dielectric data for x=0-1.0 [after Choi et al. (2005)]. (b) Room temperature structure and variation of lattice parameters of (1-x)Bi($Ni_{1/2}Ti_{1/2}$)O_3-x$PbTiO_3$ with increasing Bi($Ni_{1/2}Ti_{1/2}$)O_3 concentration [after Hu et al. (2010)].

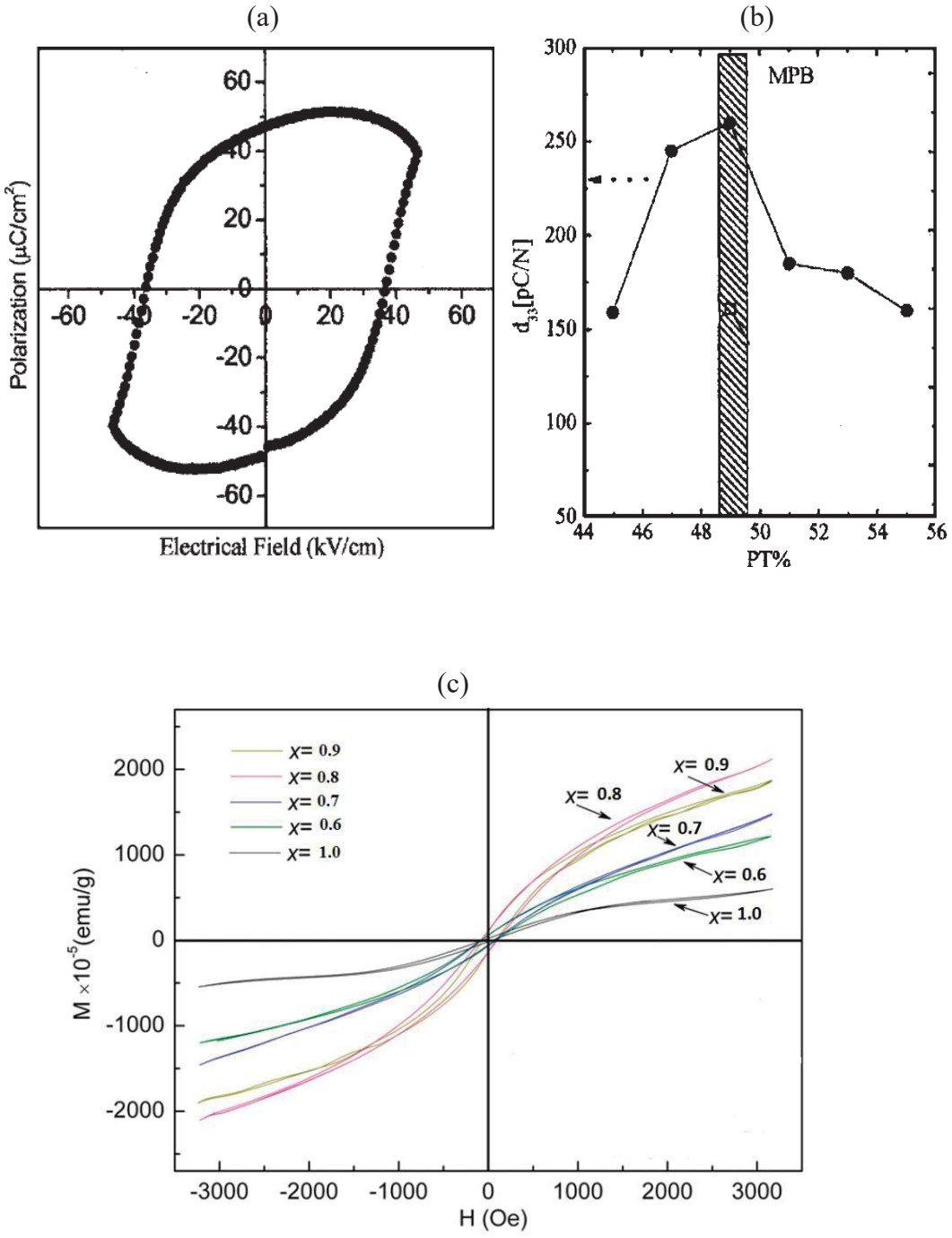

Fig.1.13. (a) P-E hysteresis loop (b) piezoelectric coefficient d_{33} for (1-x)$Bi(Ni_{1/2}Ti_{1/2})O_3$-x$PbTiO_3$ solid solution [after Choi et al. (2005)]. (b) M-H hysteresis for (1-x)$Bi(Ni_{1/2}Ti_{1/2})O_3$-x$PbTiO_3$ solid solution [after Hu et al. (2010)].

phase multiferroic systems unsuitable for potential device applications at ambient conditions. Multiferroic composites may be the solution for room temperature multiferroic with good response. Ferroelectric and magnetic phases both does not exhibit the ME response independently but the composite shows the ME property in the combined phase. The essential requirement for the composite formation is: (i) both the phases should be stable in composite form (ii) good mechanical contact in between grains (iii) high piezoelectric/magnetostrictive coefficient of component phases and (iv) high resistivity [Skinner et al. (1978); Patil et al. (2007)]. Using the concept of phase connectivity between component phases, structure of composite can be describe in 10 different ways using the notations as 0-0, 0-1, 0-2, 0-3, 1-1, 1-2, 1-3, 2-2, 2-3 and 3-3. The simplest 0-3 type composite can be fabricated by dispersing piezoelectric ceramic powders (0) uniformly in a magnetic matrix (3) [Uchino (2000)].

1.17 Multiferroic Particulate Composites

Recently, multiferroics composites have attracted considerable interest due to presence coupled ferroelectric and magnetic responses leading to magnetoelectric (ME) coupling [Eerenstein et al. (2006)]. As discussed in earlier Sections, most of the multiferroics synthesized in the form of single phase till date exhibit very low ME coefficient and are unsuitable for device applications. Further, the single phase multiferroics show the ME effect well below room temperature and therefore cannot be used for room temperature application. These drawbacks of single phase multiferroics compel the researchers to investigate attractive materials which exhibit high ME response at ambient

temperature. Concept of magnetoelectric composite formation is not very old. In 1972, Suchleten et al. (1972) introduced the concept of multiferroic composites and proposed that composites may be the better substitute for single phase multiferroics [Nan et al. (2008)]. In the multiferroic composites, both ferroelectric and magnetostrictive phases are present as independent phase. ME property in the composites appear as multiplicative property mediated by strain in response to the ferroelectric and magnetic phases. On application of the magnetic field, magnetostrictive magnetic phase changes the shape and generates strain. The developed strain in this phase is transformed to the piezoelectric phase due to the mechanical contact, which results in the polarization in the piezoelectric phase, and vice versa. [Nan et al. (2008)]. The direct and converse ME effect in the multiferroic composites is defined in equation (1.7) and (1.8), respectively as [Nan (1994)]

$$\text{Direct ME effect} = \frac{Magnetic}{\text{Mechanical}} \times \frac{Mechanical}{Electrical} \quad \text{.....(1.8)}$$

$$\text{Converse ME effect} = \frac{Electrical}{\text{Mechanical}} \times \frac{Mechanical}{Magnetic} \quad \text{.....(1.9)}$$

Since, ME coupling in composites is induced mechanically by strain, a ferroelectric system with larger tetragonality is required for the best coupling between the two phases. In the particulate composite ME coupling take place at

the interface of the grains which may not be very perfect during sintering. However, in the thin film, ME coupling take place at the atomic interfaces. It is the reason why laminated composite exhibits significantly higher ME response.

1.18 Requirement of Multiferroic Composites

Multiferroic composite can be form by taking the suitable composition of ferroelectrics and magnetic phases. To prepare composites, calcined powders of both ferroelectrics and magnetic phases are mixed and then sintered at high temperature to get the magnetoelectric coupling. The sintering temperature is controlled in such way that both phases should not react.

1.19 Structure of $Ni_{1-x}Zn_xFe_2O_4$

In the present study, we have synthesized the multiferroic composite of $0.51Bi(Ni_{1/2}Ti_{1/2})O_3$-$0.49PbTiO_3$ (BNT-PT) and $Ni_{0.6}Zn_{0.4}Fe_2O_4$ (NZFO). Our structural study reveals the enhancement in tetragonality of BNT-PT with increasing the fraction of NZFO in the composite. Large tetragonality may produce the huge strain and promise for strong coupling between two phases. $Ni_{1-x}Zn_xFe_2O_4$ has spinel (AB_2O_4) structure. The crystal structure of spinels was first resolved by Bragg [Bragg (1915)] and Nishikawa [Nishikawa (1915)]. In the crystal structure of AB_2O_4 spinels, one-eighth of the tetrahedral (named as A-sites) and one-half of the octahedral (named as B-sites) sites are occupied by cations in the cubic close-packed (fcc) array of O atoms. The unit cell contains eight A sites, 16 B-sites and 32 oxygens in the space group $Fd\bar{3}m$ [Smit and Wijn (1961)]. O-atoms in the spinel structure are not situated at the exact fcc positions. Positions of O-atoms in the unit cell are determined by a ‘u’ parameter. An ideal

close-packed arrangement has u=0.375. Hill et al. [Hill et al. (1979); Valenzuela (1994)] reported the ideal value of u=0.25 by using the origin at (0.125, 0.125, 0.125). $Ni_{1-x}Zn_xFe_2O_4$ is a mixed type spinel in which Fe^{3+} ion occupies both tetrahedral as well as octahedral positions in the unit cell. In the spinel structure of $Ni_{1-x}Zn_xFe_2O_4$, Zn^{2+}/Fe_I^{3+} ions go to the tetrahedral sites 8(a) at (1/8, 1/8, 1/8), Ni^{2+}/Fe_{II}^{3+} ions octahedral sites 16(d) at (1/2, 1/2, 1/2) and O^{2-} ions at 32(e) sites (x, x, x).

Spinels are categorized as normal, inverse and mixed types on the basis of cationic distribution. $NiFe_2O_4$ is an example of inverse spinel while $ZnFe_2O_4$ is a normal spinel. Ni-Zn ferrite with general formula $Ni_{1-x}Zn_xFe_2O_4$ is the most widely studied spinel in which solid solution can be formed by varying the concentration of Zn as $0 \leq x \leq 1$. Increasing the concentration of Zn significantly modify the lattice parameters as well as magnetic structure of $NiFe_2O_4$ due to the larger size of Zn^{2+} (0.60Å) than Fe^{3+} (0.49Å) [Shannon and perwitt (1976); Valenzuela (1994)]. The variation of lattice parameters with dopant Zn is shown in Fig.1.14. Lattice parameters enhance with increasing the concentration of Zn without any modification in the crystal symmetry which remain cubic with space group $Fd\bar{3}m$.

1.20 Magnetic Properties of $Ni_{1-x}Zn_xFe_2O_4$

$NiFe_2O_4$ is an example of inverse spinel whose magnetic character is greatly influenced by substitution of Zn, Cd or other cations at Ni site. Ferrimagnetic nature is observed in the pure $NiFe_2O_4$ at room temperature. Substitution of Zn at Ni site in $Ni_{1-x}Zn_xFe_2O_4$ completely changes the magnetic

behaviour. The net magnetic moment (μ_B) of $Ni_{1-x}Zn_xFe_2O_4$ increases with increasing the concentration of Zn, depicts a maxima for intermediate compositions and then decreases as shown in Fig.1.15. Zn^{2+} is a diamagnetic cation and breaks the interaction linkage between magnetic ions. Zn^{2+} has larger ionic radii than Ni^{2+} and Fe^{3+} which increases the cell parameter of cubic unit cell after substitution and thus magnetic structure of $Ni_{1-x}Zn_xFe_2O_4$. Spin arrangements of $Ni_{1-x}Zn_xFe_2O_4$ with increasing the concentration of Zn^{2+} ions are shown in Fig.1.16. $Ni_{1-x}Zn_xFe_2O_4$ reveals ferrimagnetic nature for the composition with $x<0.4$, triangular or Yafet-Kittel (1952) type behaviour for $x>0.5$ and antiferromagnetic character around the compositions with $x=1.0$ [Valenzuela (1994)]. This relationship is not followed over the entire composition range. As Zn content increases, A-O-B interactions become too weak and B-O-B interactions begin to dominate. Instead of a collinear, antiparallel alignment, a canted structure appears where spins in B sites are no longer parallel. Evidence of this triangular structure has been observed by neutron diffraction [(Satyamurthy et al. (1969); Yafet and Kittel (1952)]. For high Zn concentration, B-O-B interactions dominate and the ferrite become antiferromagnetic [Boucher et al. (1970)]. Fig.1.17. shows the variation of Curie temperature with composition (x) for the $Ni_{1-x}Zn_xFe_2O_4$. Curie temperature decreases significantly with increasing the concentration of Zn ions. Curie temperature for $x=0.1$ is 800K which approaches to 100K for $x=0.9$ [Globus et al. (1977)].

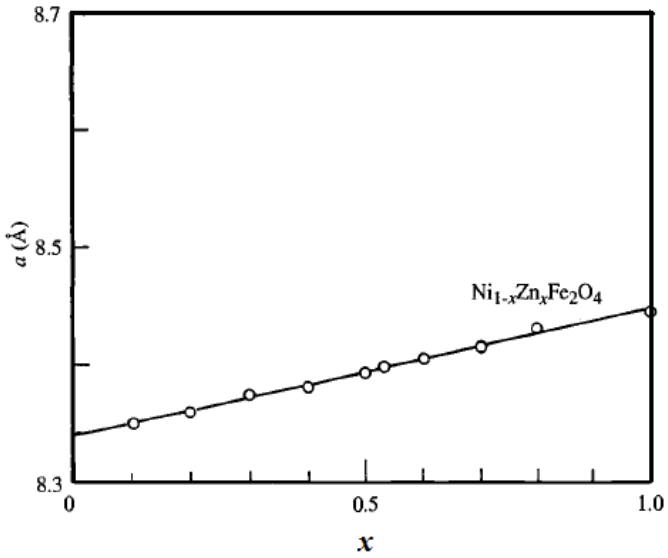

Fig.1.14. Variations of lattice parameter for $Ni_{1-x}Zn_xFe_2O_4$ with x [after Globuset al. (1977); Valenzuela (1994)].

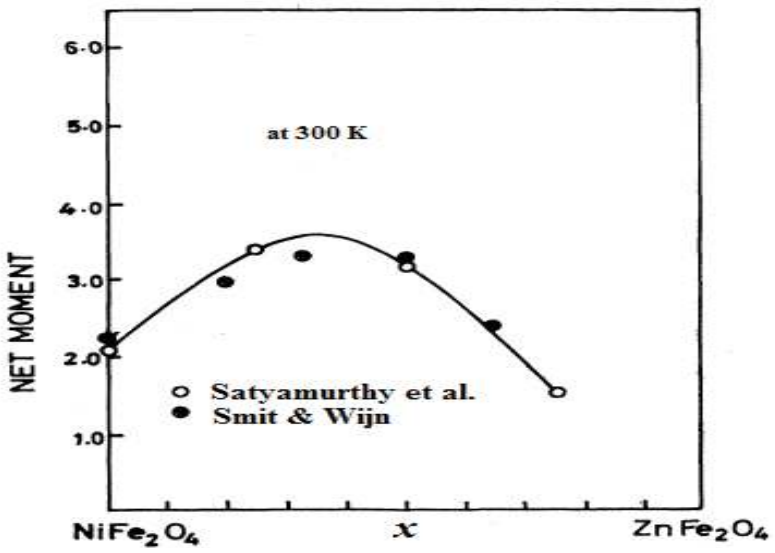

Fig.1.15. Net magnetic moments (circle) of $Ni_{1-x}Zn_xFe_2O_4$ at room obtained after magnetic refinement of neutron data [after Satyaurthy et al. (1969)]. Black dots are the net magnetic moments obtained by Smit and Wijn [after Smit and Wijn (1961)].

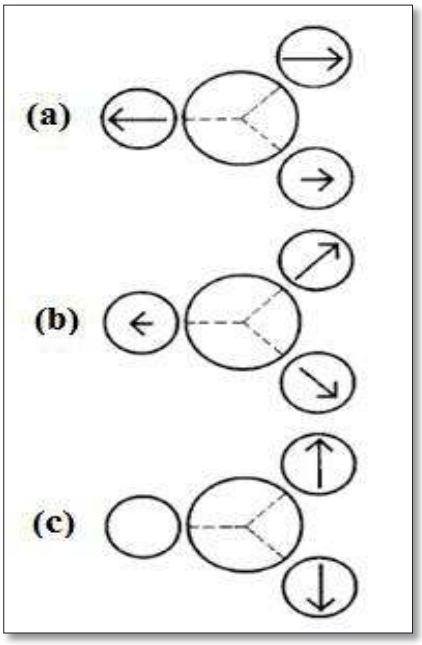

Fig.1.16. Various types of spin arrangements and resultant magnetic interactions in $Ni_{1-x}Zn_xFe_2O_4$ with increasing the concentration of Zn (a) Ferrimagnetic for the compositions with $x<0.4$ (b) Triangular or Yafet-Kittel type for the compositions with $x>0.5$ and (c) antiferromagnetic for the compositions close to x=1.0 [after Valenzuela (1994)].

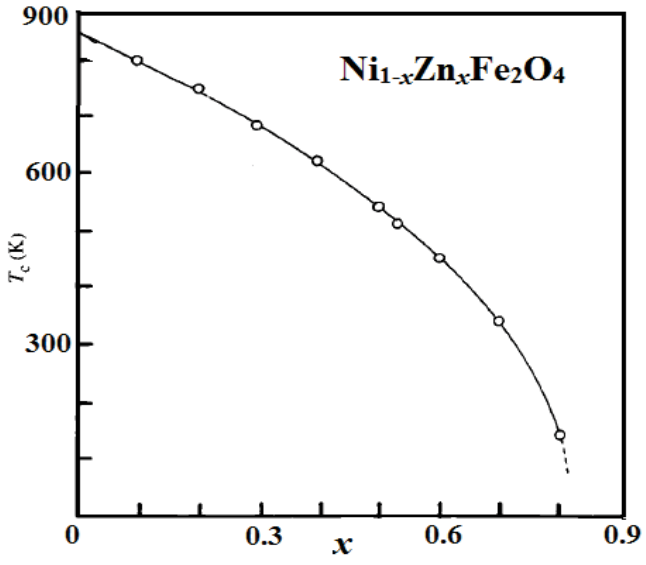

Fig.1.17. Variations of Curie temperature with composition (x) for the $Ni_{1-x}Zn_xFe_2O_4$ solid solution [after Globus et al. (1977)].

1.21 Magnetoelectric Coupling in Particulate Composites

The magnetoelectric property originates from the elastic coupling between magnetostrictive and piezoelectric materials in composites, scientists in the Philips Laboratory synthesized the composite of $BaTiO_3/CoFe_2O_4$ and found large ME coefficient ~ 0.13V/cm-Oe. The value of ME coefficient in $BaTiO_3/CoFe_2O_4$ is hundred times higher than single phase materials [Skinner et al. (1978); Nan et al. (2008); Boomgard et al. (1974); Run et al. (1974); Boomgard et al. (1976); Boomgard and Born (1978); Harshe et al. (1993)]. A surge of interest in multiferroic composites was started around (2000) when very high ME-coefficient was observed in laminate composite [Mathe et al. (2000)]. If the magnetic field is applied on magnetic materials then $\partial S/\partial H=e^m$ and $\partial P/\partial S=e$ on applied electric field, where S is the strain, e^m and e are magnetostrictive and piezoelectric coefficients. In the two phase composite materials which are formed by piezoelectric and magnetostrictive phases $\partial P/\partial H=\alpha=k_c\, e^m\, e$, where k_c is a coupling factor $0\leq|k_c|\leq1$ between the two phases, [Nan (2008); Nan (1993)] and α is the ME coefficient of the composite. *kc* is a coupling factor between the two phases [Nan (1993)]. Magnetoelectric coupling in the composites has been described in the framework of Green's function and perturbation theory [Nan (1994); Nan and Clarke (1997)]. For the magnetoelectric composites which are formed by elastic interaction between magnetostictive and piezoelectric phases, corresponding equation describing the mechanical-electric-magnetic [Nan et al. (2008); Nan (1994)] coupling response in magnetoelectric composites can be written in tensor form as

$$\boldsymbol{\sigma = c\,S - e^{T}\,E - q^{T}\,H} \quad \ldots\ldots\ldots\ldots \quad (1.10)$$

$$\boldsymbol{D = e\,S + \varepsilon\,E + \alpha\,H} \ldots\ldots\ldots\ldots\ldots \quad (1.11)$$

$$\boldsymbol{B = q\,S + \alpha^{T}\,E + \mu\,H} \ldots\ldots\ldots\ldots\ldots \quad (1.12)$$

where, $\boldsymbol{\alpha}$ is the ME-coefficient tensor, $\boldsymbol{\alpha^{T}}$ transpose of $\boldsymbol{\alpha}$, $\boldsymbol{\sigma}$ stress, **S**, **D**, **E**, **B**, and **H** are the stress, strain, electric displacement, electric field, magnetic induction, and magnetic-field, respectively. **c**, $\boldsymbol{\varepsilon}$, $\boldsymbol{\mu}$ are, respectively, the stiffness, dielectric constant, and permeability, **e** ($\mathbf{e^{T}}$) and **q** are the piezoelectric and piezomagnetic coefficients, respectively. The quantities **c**, **e**, **q**, $\boldsymbol{\varepsilon}$ and $\boldsymbol{\mu}$ are the tensor of rank (6x6), (3x6), (3x6), (3x3), (3x3) and (3x3). Equations (1.10), (1.11) and (1.12) can be solved with the help of Green's function. Resultant ME-coefficient comes out [Nan (1994)]

$$\boldsymbol{\alpha^{*} = <(e^{*} - e)T^{13}><T^{33}>^{-1} = <(q^{*} - q)T^{12}><T^{22}>^{-1}} \ldots\ldots\ldots(1.13)$$

where asterisk (*) denotes the average value. T^{ij} is called the t-matrix.

Different types of particulate and laminate composites such as $Tb_{1-x}Dy_xFe_2$(Terfenol-D)/PZT, Terfenol-D/PVDF, Terfenol-D/P(VDF-TrFE) etc were synthesized recently which exhibit giant ME-response. Nanostructured composite thin films of magnetic and ferroelectric oxides have been shown great interest. Zheng et al. [Zheng et al. (2004); Nan et al. (2008)] have reported important works on nanostructured thin film $BaTiO_3/CoFe_2O_4$ composite. Recently, nanostructured thin film multiferroic composites are the hot topic of

experimental and theoretical study [Ramesh and Spaldin (2007)] which are promising materials for application in microelectronic device [Nan et al. (2008)].

Fig.1.18 shows the ME-coefficient of (1-x)$Na_{0.5}Bi_{0.5}TiO_3$/x$MnFe_2O_4$ (NBT/MFO) composite [Praveena and Varma (2014)]. ME-coefficient is nearly constant for the different compositions of NBT/MFO. The ME effect in the composites results from the multiplicative property of piezoelectric and magnetostrictive phases. Magnetostrictive property associated with the movement of domains which spontaneously deformed in the direction of applied field [Kingery 1988; Nan et al. (2001)]. Variations of ME-coefficient for (x)$NiFe_2O_4$/(1-x)$Ba_{0.8}Sr_{0.2}TiO_3$ composites is shown in Fig.1.19. ME-coefficient decreases with increasing the applied DC field. At higher applied (DC) field, magnetostrictive property and thus output voltage get saturated which results in to decrease in (dE/dH) ME-coefficient [Patil et al. (2007); Cai et al. (2003)].

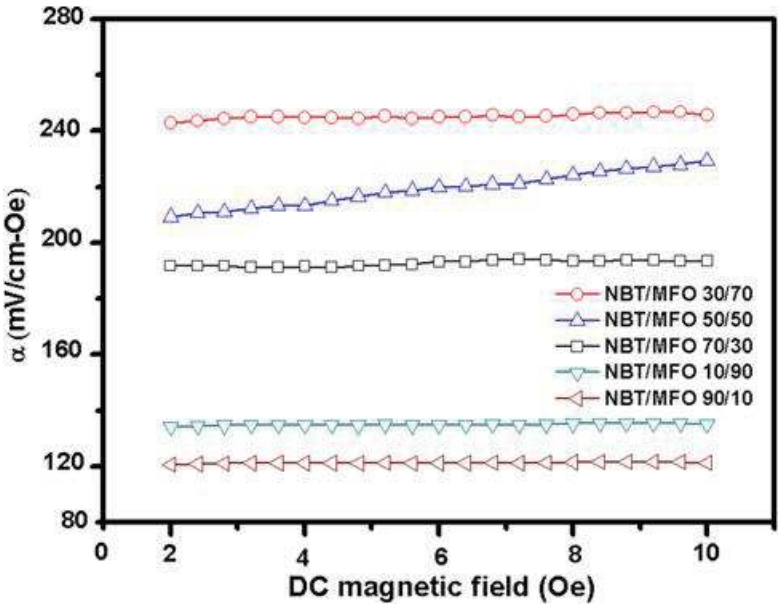

Fig.1.18. Variations of ME-coefficient (α=dE/dH) in $Na_{0.5}Bi_{0.5}TiO/MnFe_2O_4$ composites at applied AC field of 3Oe [after Praveena and Varma (2014)].

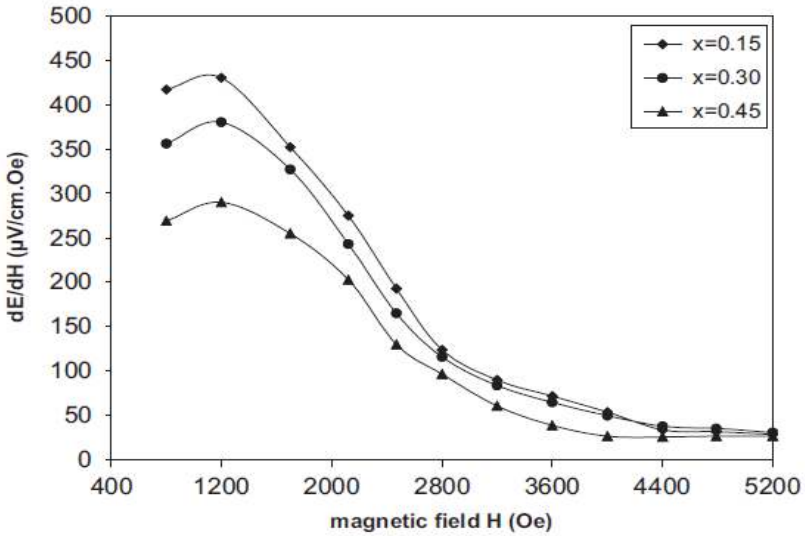

Fig.1.19. Variations of ME-coefficient (α=dE/dH) for $(x)NiFe_2O_4/(1-x)Ba_{0.8}Sr_{0.2}TiO_3$ composites sintered at 1200^0C for 12 hours [after Patil et al. (2007)].

1.22 Objective of the Present Thesis Work

The main objectives of the present work on the (1-x)BNT-xPT solid solutions are as follow:

1. To synthesize phase pure perovskite solid solution of $Bi(Ni_{1/2}Ti_{1/2})O_3$ and $PbTiO_3$.

2. To study the room temperature crystal structure of (1-x)$Bi(Ni_{1/2}Ti_{1/2})O_3$-x$PbTiO_3$ solid solution over the entire composition range.

3. To study the effect of $PbTiO_3$ substitution on the ferroelectric properties of $Bi(Ni_{1/2}Ti_{1/2})O_3$ over the entire composition range.

4. To understand the nature of phase transition at high as well as low temperature in (1-x)$Bi(Ni_{1/2}Ti_{1/2})O_3$-x$PbTiO_3$ ceramics.

5. To study the effect of $PbTiO_3$ substitution on the sequence of high temperature phase transitions of BNT.

6. To study the magnetoelectric response of (1-y)0.51$Bi(N_{i1/2}T_{i1/2})O_3$-0.49$PbTiO_3$/y$N_{i0.6}Z_{n0.4}Fe_2O_4$ composite.